Journal of Thermal Analysis and Calorimetry, Vol. 73 (2003) 895–902

RARE EARTH COMPLEXES WITH 4-METHYLMORPHOLINE-N-OXIDE
Synthesis, characterization and kinetics of thermal decomposition

A. M. Garrido Pedrosa[*]*, M. S. C. Câmara, F. M. M. Borges,*
H. K. S. de Souza, H. Scatena Jr., D. M. A. Melo and L. B. Zinner

Federal University of Rio Grande do Norte, Department of Chemistry, C.P. 1662, 59078-970 Natal, RN, Brazil

(Received October 27, 2002; in revised form February 9, 2003)

Abstract

Complexes of rare earth trifluoroacetates (TFA) with 4-methylmorpholine-N-oxide (MMNO) of composition $\mathrm{Ln(TFA)_3{\cdot}3MMNO}$ (*Ln*=Eu, Dy, Ho, Er, Yb and Y) were synthesized and characterized by elemental analysis data, complexometric titration with EDTA, IR absorption spectra, thermogravimetric analyses and differential scanning calorimetry (DSC) in N_2 atmosphere. Infrared spectroscopy data revealed that the MMNO molecules are bound to the central ion through the oxygen of NO groups. These data suggest that the trifluoroacetate groups are also coordinated. Thermogravimetric curves indicate that the decomposition of MMNO begins at approximately 350 K and results in Ln_2O_3 residue at around 1170 K. A theoretical kinetic study was carried out using a QBASIC program with the TG input data for the Dy complex.

Keywords: kinetics, 4-methylmorpholine-N-oxide, rare earth complexes, thermal decomposition, trifluoroacetates

Introduction

The synthesis, characterization and kinetic thermal decomposition of rare earth complexes have been extensively studied [1–5]. These complexes decompose at moderate temperatures, usually giving metallic oxides, pure metal and/or inorganic salts as final product. The composition of the final product depends on variables such as the decomposition atmosphere (oxidizing, reducing or inert), the organic ligands, central atom, etc. Although rare earth complexes containing 4-methylmorpholine-N-oxide (MMNO) as neutral ligand have been extensively studied [6–11], data on rare earth trifluoroacetates with such ligand are still scarce. Trifluoroacetates can be monodentate or bidentate ligands, or even act as a bridge between two central atoms, also either not coordinated [12].

---

[*] Author for correspondence: E-mail: annemgp@yahoo.com

1388–6150/2003/ $ 20.00

Akadémiai Kiadó, Budapest
Kluwer Academic Publishers, Dordrecht

The purpose of this study was to synthesize, characterize and determine the kinetic parameters of thermal decomposition of rare earth trifluoroacetate complexes with 4-methylmorpholine-N-oxide (MMNO) using the thermogravimetric curve of the Dy complex. Several authors have studied ways to obtain kinetic parameters from the measured TG curves with minimum uncertainty [13–15]. In this work, this was possible by simulating TG curves using a QBASIC program and correlating them to the measured thermogravimetric data.

Experimental

The complexes were prepared by the reaction of hydrated rare earth trifluoroacetates with MMNO in methanol (molar ratio 1:3). Carbon, hydrogen and nitrogen content was determined using a Perkin Elmer CHN analyzer model 240. IR spectra were performed on a FT-IR Prospect MIDAC apparatus, using KBr pellets. X-ray powder diffraction patterns were determined using a Rigaku RU-200B diffractometer employing CuK_{α} radiation. Thermogravimetric curves were obtained on a Perkin Elmer TGA-7 instrument at a heating rate of 5 K min^{-1} in nitrogen flowing at a rate of 50 cm^3 min^{-1}. DSC curves were obtained using a Shimadzu DSC 50 instrument in N_2 atmosphere (heating rate 5 K min^{-1} and gas flow of 50 cm^3 min^{-1}). Kinetic parameters were obtained by simulating TG curves using the equations presented in this paper.

Results and discussion

The analytical results in Table 1 indicate the formula $Ln(TFA)_3\cdot 3MMNO$ (*Ln*=Eu, Dy, Ho, Er, Yb and Y; *TFA*=trifluoroacetate and *MMNO*=4-methylmorpholine-N-oxide). IR absorption spectra suggest that MMNO is coordinated through the O-atom of the NO group and indicate that the trifluoroacetate counter-ions are bonded to the central ion as monodentate or bidentate ligands, or even act as bridges between two lanthanide ions (Table 2). X-ray powder patterns are identical, indicating the formation of an isomorphous series [9].

Table 1 Analytical results of $Ln(TFA)_3\cdot 3MMNO$ complexes

Ln	Ln/%		C/%		H/%		N/%	
	theor.	exp.	theor.	exp.	theor.	exp.	theor.	exp.
Eu	18.7	18.4	29.9	29.5	3.9	4.2	4.9	4.8
Dy	19.1	19.1	29.6	29.8	3.9	3.9	4.9	4.9
Ho	19.2	19.3	29.5	30.3	3.9	4.1	4.9	5.2
Er	19.5	20.2	29.4	28.7	3.8	3.6	4.8	4.7
Yb	20.0	20.6	29.2	28.3	3.8	3.8	4.9	4.6
Y	11.4	11.5	32.2	31.6	4.2	4.1	5.4	5.3

Table 2 Infrared absorption frequencies (cm^{-1}) relative to the $Ln(TFA)_3 \cdot 3MMNO$ complexes, anion and 4-methylmorpholine-N-oxide

Ln	NO	COC	$\nu_{as}COO^-$	ν_sCOO^-	δCOO^-
Eu	966	1207	1694	1459	721
Dy	966	1207	1698	1459	721
Ho	965	1195	1689	1456–1428	721
Er	965	1198	1715–1691	1459–1429	721
Yb	964	1198	1720–1691	1464–1429	721
Y	965	1203	1718–1692	1461–1430	721
MMNO	937	1176	–	–	–
TFA	–	–	1666	1469	728

Thermogravimetric curves were recorded to evaluate the thermal stability of the complexes and to assist the kinetic study. The heating rate and atmosphere were chosen according to preliminary investigations [9]. Figure 1 shows the TG curves of selected $Ln(TFA)_3 \cdot 3MMNO$ (*Ln*=Dy and Er) obtained in N_2 atmosphere, at 5 K min^{-1} and Table 3 summarizes the thermogravimetric data of the complexes.

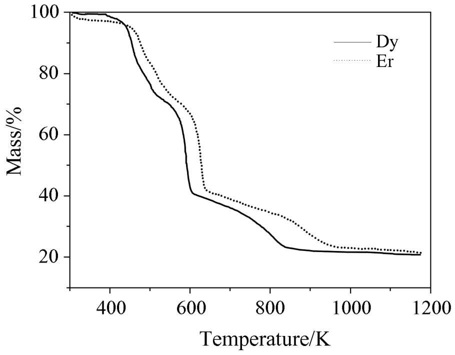

Fig. 1 Thermogravimetric curves of $Ln(TFA)_3 \cdot 3MMNO$ (*Ln*=Dy and Er), recorded in dynamic N_2 atmosphere (50 cm^3 min^{-1}) and heating rate of 5 K min^{-1}

The first step of the thermal decomposition occurs at about 349 K with the onset of MMNO decomposition. Full decomposition of MMNO takes place between 543 and 682 K along with the decomposition of TFA evolving gaseous products, especially CO, CO_2, CF_3OF and $(CF_3CO)_2O$ [16]. The decomposition of TFA continues up to 1170 K, with the formation of lanthanide oxide (Ln_2O_3) as a final residue.

Table 4 summarizes the enthalpy change and temperature range of the decomposition of the complexes. DSC curves of $Ln(TFA)_3 \cdot 3MMNO$ (*Ln*=Dy, Er and Y) (Fig. 2) show that the decomposition of MMNO and TFA are both exothermic for the complexes of Eu, Yb or Y. On the other hand, complexes containing Dy, Ho or Er, MMNO decomposed both endothermically and exothermically, whereas TFA decomposed exothermically.

Table 3 Summary of thermal decomposition of the Ln(TFA)$_3$·3MMNO complexes, in N_2 flow (50 cm^3 min^{-1}) and heating rate of 5 K min^{-1}

Ln	Temperature range/K				Mass loss/%			
	I	II	IIII	residue	I	II	IIII	residue
Eu	363–545	545–651	651–1170	1170	21.3	39.2	19.1	20.4
Dy	369–543	543–659	659–1170	1170	28.7	32.3	17.5	21.5
Ho	353–546	546–682	682–1170	1170	22.8	37.6	16.6	23.0
Er	349–546	546–682	682–1170	1170	26.8	34.5	14.9	23.8
Yb	353–573	573–679	679–1170	1170	28.0	30.1	19.0	22.9
Y	361–587	587–660	660–1170	1170	34.2	29.8	23.1	12.9

Table 4 Thermodynamic parameters of thermal decomposition of the Ln(TFA)$_3$·3MMNO complexes, in flowing N_2 (50 cm^3 min^{-1}) and heating rate of 5 K min^{-1} from DSC measurements

Ln	Stage of decomposition					
	I		II		III	
	Peak/K	Δ*H*/kJ mol^{-1}	Peak/K	Δ*H*/kJ mol^{-1}	Peak/K	Δ*H*/kJ mol^{-1}
Eu	428	381	572	236	–	–
Dy	348	41	436	496	559	99
Ho	351	31	441	325	589	203
Er	340	22	448	436	588	225
Yb	433	246	576	125	–	–
Y	435	443	580	229	–	–

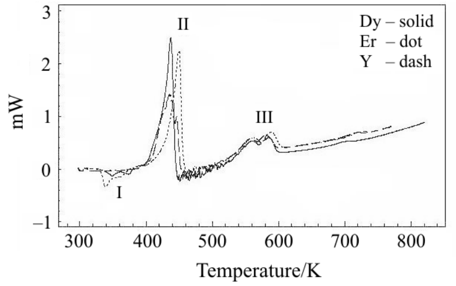

Fig. 2 DSC curves of the Ln(TFA)$_3$·3MMNO (*Ln*=Dy, Er and Y), recorded in dynamic N_2 atmosphere (50 cm^3 min^{-1}) and heating rate of 5 K min^{-1}

The kinetic parameters were calculated by a QBASIC program using the obtained TG data of the Dy(TFA)$_3$·3MMNO decomposition. This curve was chosen for the determination of kinetic parameters as its decomposition steps are quite well separated. A simulation of the thermogravimetric data was carried out and the following kinetic equation:

$$\Delta m_{\mathrm{i,j}} = -k_{0,\mathrm{i}}\exp\left(-\frac{E_{\mathrm{ai}}}{RT}\right)\Delta m_{\mathrm{i,j-1}}\Delta t_{\mathrm{j}} + \frac{M_{\mathrm{i+1}}}{M_{\mathrm{i}}}\Delta m_{\mathrm{i,j-1}} \qquad (1)$$

where $m_{\mathrm{i,j}}$ represents the mass increment of the *i*-th compound at the *j*-th step, $k_{0,\mathrm{i}}$ is the pre-exponential factor, $E_{\mathrm{a,i}}$ is the activation energy of the *i*-th processes, $M_{\mathrm{i,j}}$ represents the molar mass of the compound *i*, Δt_{j} the time increment of the *j*-th step and $\Delta m_{\mathrm{i,j-1}}$ the mass increment of the previous step.

The initial mass of the first component is the initial mass, m_1, of the original sample. For the other components the initial mass is zero. Using a set of activation energy and pre-exponential factor, it is possible to visually approximate the theoretical mass change to the experimental one. The theoretical mass is given by:

$$m_{\mathrm{j}} = \sum_{\mathrm{i}} m_{\mathrm{i,j}} \qquad (2)$$

where m_{j} is the total mass at the *j*-th step.

Reaction of the first order was proposed. The quality of the theoretical approach to fit the observed curve is visually established. The first and second derivatives of TG curves are particularly helpful for this purpose.

The developed computer program minimizes the value of the function

$$\sum_{j=1}^{N}\left(1-\frac{m_{\mathrm{sim,j}}}{m_{\mathrm{exp,j}}}\right)^2 \tag{3}$$

where $m_{\mathrm{exp,j}}$ and $m_{\mathrm{sim,j}}$ are experimental and the simulated mass at the j-th step.

This function was minimized using a visual optimization method superimposing the experimental and simulated curves. In order to assist the fitting procedure, both the first and second derivative curves were employed. The graphic of $m_{\mathrm{sim,j}}$ as a function of $m_{\mathrm{exp,j}}$ (Fig. 3) was included and it presented an R=0.99978 of the integral curve suggesting that such approach is promising.

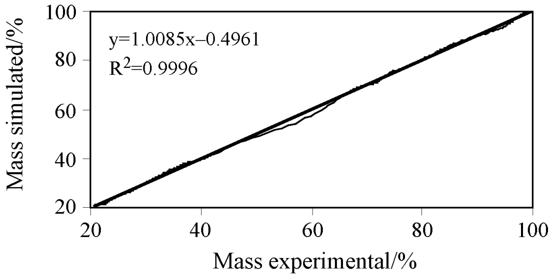

Fig. 3 Correlation of the mass experimental and simulated for Dy(TFA)$_3$·3MMNO, obtained from TG data and kinetic study

Table 5 Kinetic parameters of thermal decomposition of the Dy(TFA)$_3$·3MMNO complex and mass percentage of intermediate products

	Stage of decomposition						
	I	II	III	IV	V	VI	VII
k_0/s^{-1}	$1.0\cdot10^{4}$	$5.5\cdot10^{4}$	$6.1\cdot10^{6}$	$1.0\cdot10^{6}$	$1.0\cdot10^{20}$	$4.0\cdot10^{4}$	$1.0\cdot10^{20}$
E_a/kJ mol^{-1}	56.0	60.0	70.0	79.0	250.0	112.5	600
m/%	100.0	95.5	94.5	80.5	70.1	40.2	21.1

Hypotheses for the molar mass of the reaction intermediates can be postulated and tested using the integral curve simulation approach. The kinetic parameters obtained from each thermal decomposition step are presented in Table 5. Figure 4 shows the simulated and experimental thermogravimetric curves for the Dy complex. Figure 5 shows the first and second derivatives of both the simulated and experimental TG curves for this complex. They are very close to experimental derivatives indicating that the proposed model, for the whole decomposition of the Dy complex is plausible. E_{ai}, $k_{0\mathrm{i}}$ and the intermediate molar masses were determined fitting the ex-

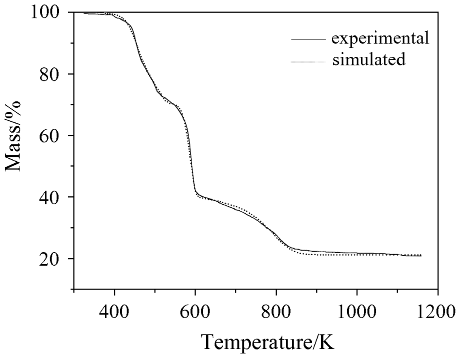

Fig. 4 Thermogravimetric curves simulated and experimental for $Dy(TFA)_3{\cdot}3MMNO$, recorded in dynamic N_2 atmosphere (50 $cm^3\ min^{-1}$) and heating rate of 5 K min^{-1}

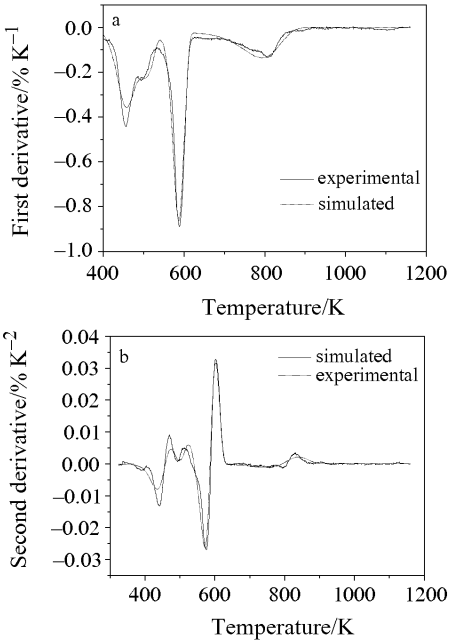

Fig. 5 First (a) and second (b) derivative TG curves (simulated and experimental) for $Dy(TFA)_3{\cdot}3MMNO$

perimental curves. Although the TG curve for this complex indicated four stages of the decomposition, nevertheless, according to the theoretical and experimental adjust of the curves (Eqs (1) to (3)) seven stages of decomposition were detected, that is, the process consisted of seven complex steps.

Conclusions

Rare earth trifluoroacetate complexes with 4-methylmorpholine-N-oxide, have not been described in the literature. The thermal characterization was carried out by TG, DSC, while the kinetic study using a QBASIC program infer the TG data as input. The proposed mechanism for the observed thermal decomposition consists of consecutive reactions of the organic intermediates. The method previously introduced [5] shows a good agreement with the plotted curves and suggests that each peak corresponds to more than one reaction. The first and second derivatives indicate the high quality of the optimization of the mass curves.

References

1 G. Vicentini, L. B. Zinner, J. Zukerman-Schpector and K. Zinner, Coord. Chem. Rev., 196 (2000) 353.

2 A. M. Garrido Pedrosa, M. K. S. Batista, F. M. M. Borges, L. B. Zinner, H. Scatena Jr. and D. M. A. Melo, Eclética Química, 27 (2002) 32.

3 G. F. Sá, O. L. Malta, C. Mello Donegá, A. M. Simas, R. L. Longo, P. A. Sant-Cruz and E. F. Silva Jr., Coord. Chem. Rev., 196 (2000) 165.

4 E. P. Marinho, F. M. M. Borges, D. M. Araújo Melo, H. Scatena Jr., L. B. Zinner and K. Zinner, Thermochim. Acta, 344 (2000) 81.

5 A. M. Garrido Pedrosa, P. M. Pimentel, D. M. A. Melo, H. Scatena Jr., F. M. M. Borges, A. G. Souza and L. B. Zinner, J. Therm. Anal. Cal., 67 (2002) 397.

6 R. F. Bezerra, D. M. Araújo Melo, G. Vicentini, K. Zinner and L. B. Zinner, J. Alloys Comp., 344 (2002) 120.

7 V. D. Santos, L. B. Zinner, K. Zinner and A. G. Silva, J. Alloys Comp., 275 (1998) 792.

8 L. C. Fernandes, R. F. Bezerra, M. S. C. Câmara, D. M. A. Melo and L. B. Zinner, An. Bras. Quim., 50 (2000) 16.

9 M. S. C. Câmara, M. Sc. Dissertation, UFRN, Natal, RN, Brazil 2000.

10 V. D. Santos, L. C. Schmitz, K. Zinner, P. C. Isolani and L. B. Zinner, J. Alloys Comp., 225 (1995) 347.

11 L. C. Fernandes, J. R. Matos, L. B. Zinner, G. Vicentini and J. Zukerman-Schpector, Polyhedron, 19 (2000) 2313.

12 F. L. Alencar, J. R. Matos and L. B. Zinner, J. Alloys Comp., 207 (1990) 461.

13 S. Vyazovkin and A. I. Lesnikovich, Thermochim. Acta, 165 (1990) 11.

14 W. W. M. Wendlandt, Thermal Analysis, 3rd Ed., Texas, Kolthoff 1964.

15 M. E. Brown, Introduction to Thermal Analysis, Techniques and Applications, Chapman and Hall, London 1988.

16 K. W. Rillings and J. C. Roberts, Thermochim. Acta, 10 (1974) 285.